脈衝星磁場球內的粒子加速

徐佩君[1]、廣谷幸一[1]、張祥光[2]
[1]高等理論天文物理研究中心
[2]清華大學物理系與天文研究所

摘要

我們討論一高轉速中子星磁場球內的粒子加速連鎖反應；全球性電流造成電荷空乏區內存在延著磁力線的強大電場，正負電子經由此電場加速幅射出伽瑪射線，某些伽瑪射線與中子星表面放出的 X 射線碰撞產生正負電子對，這些帶電粒子屏蔽了部分原來的電場，所有物理過程都須同時考慮。此篇論文中，我們首次討論粒子加速區隨時間演化的性質，藉由同時解 Poisson 方程與正負電子及光子的 non-stationary Boltzmann 方程。將此方法應用至毫秒脈衝星上，考慮磁極冠表面被往回流的加速粒子撞擊加熱，我們發現對於一定範圍的毫秒脈衝星參數（自轉週期、週期微分、磁傾角），解會收斂爲穩定解，此時粒子加速連鎖反應藉由磁極冠的熱輻射維持。檢驗一加速區是否能自我維持，我們訂出毫秒脈衝星在週期-週期微分圖上對於幾個不同磁傾角的死亡線。

Particle Acceleration in Pulsar Magnetospheres

Pei-Chun Hsu[1], Kouichi Hirotani[1], Hsiang-Kuang Chang[2]
[1] ASIAA/National Tsing Hua University-TIARA
[2] Department of Physics & Institute of Astronomy, National Tsing Hua University

Abstract

We investigate a pair creation cascade in the magnetosphere of a rapidly rotating neutron star. The charge depletion due to global flows of charged particles causes a large electric field along the magnetic field lines. Electrons and positrons are accelerated by this field to radiate gamma-rays via curvature process. Some of the gamma-rays collide with the X-rays emitted from the stellar surface to materialize as pairs in the gap. The replenished charges partially screen the original electric field. To take in to account of these physical processes self-consistently, we solve the set of the Poisson equation for the electro-static potential and the Boltzmann equations for electrons, positrons, and gamma-ray photons simultaneously. In this paper, we first examine the time-dependent nature of particle accelerators by solving the non-stationary Boltzmann equations on the two-dimensional poloidal plane in which both the rotational and magnetic axes reside. Evaluating the temperature of the heated polar cap surface, which is located near the magnetic pole, by the bombardment of gap-accelerated particles, and applying the scheme to millisecond pulsar parameters, we

demonstrate that the solution converges to a stationary solution of which pair-creation cascade is maintained by the heated polar-cap emission, in a wide range of three-dimensional parameter space (period, period derivative, magnetic inclination angle). We also present the deathlines of millisecond pulsars.

關鍵字（Keywords）：伽瑪射線（gamma-rays: theory）、數值方法（methods: numerical）、脈衝星（pulsars: general）

Received: 2006.10.01; accepted: 2006.10.26

1. Introduction

The Energetic Gamma-Ray Experiment Telescope (EGRET) on the Compton Gamma Ray Observatory (CGRO) had detected gamma-ray pulsed emissions from seven pulsars. The light curves and spectra of these gamma-ray pulsars enable us to understand the γ-ray emission mechanism and examine different models. The prospective γ-ray telescope such as Gamma-ray Large Area Space Telescope (GLAST) will provide more γ-ray observation with higher sensitivity. The origin of gamma-ray emission from pulsar magnetosphere will be studied more thoroughly.

To emit γ-ray emission with energy above GeV, the charged particles in the pulsar magnetosphere have to be accelerated to relativistic energy. The location and mechanism of particle acceleration and γ-ray emission have not been completely understood. Many models have been presented to explain the gamma-ray emission from the potential drop, or the gap, formed in the open zone. In polar cap models, or equivalently inner-gap models (Harding, Tademaru, & Esposito 1978; Daugherty & Harding 1982, 1996; Dermer & Sturner 1994; Sturner, Dermer, & Michel 1995), the production of γ-ray radiation is within several neutron star radii over a pulsar polar cap surface. On the other hand, outer gap models (Cheng, Ho & Ruderman 1986a, b; Chiang & Romani 1992, 1994; Romani & Yadigaroglu 1995) consider radiation in the outer part of magnetosphere. Both of these two models have successfully explained many properties of observed light curves or spectra. However, no model can perfectly reproduce properties of both light curves and spectra simultaneously.

Base on the work Cheng, Ho & Ruderman (1986a,b), the three-dimensional outer gap models (Romani & Yadigaroglu 1995; Cheng, Ruderman and Zhang 2000) can successfully explain the observed light curve in reproducing the wide separation of the two peaks with bridge emission. Dyks and Rudak (2003) found that radiation region with inner boundary extended toward the stellar surface can explain the off- pulse emission, which cannot be reproduced by a traditional outer gap. A one-dimensional model of an outer gap with electrodynamical approach was investigated (Hirotani & Shibata 1999a,b,c; Hirotani, Harding

& Shibata 2003). They solved accelerating electric field, curvature radiation, and pair creation processes self-consistently. The model spectra can fit Vela observation well at 100 MeV - 10 GeV. In their model, it was analytically demonstrated that an active gap, which must be non-vacuum, possesses a qualitatively different properties from the vacuum solution of traditional outer-gap models. It was shown that the inner boundary of the outer gap shifts toward the stellar surface as the created current increases.

Subsequently, Takata, Shibata, and Hirotani (2004) and Takata et al. (2006) studied the two-dimensional model which takes the trans-field structure into account. Solving the Poisson equation for the electrostatic potential on the two-dimensional poloidal plane, they revealed that the gap inner boundary is located inside of the null surface because of the pair creation within the gap. In their model, it is assumed that the particle motion immediately saturates in the balance between electric and radiation-reaction forces. However, there are cases in which particles run a good fraction of the whole gap length until they achieve the saturation. On these grounds, we solve the unsaturated particle momenta and pitch angle evolution with synchrotron-curvature radiation in the two-dimensional geometry and we will discuss the particle motion and the electric field structure of the outer gap in this paper.

The high energy emission from millisecond pulsars (MSPs) is another important issue. Up to now, there are 28 MSPs having detected X-ray emission. Six among them have pulsed X-ray emission. These six X-ray MSPs can be divided into two classes by their observational X-ray properties (Kuiper et al. 2000). The Class-I members (PSR J0437-4715, PSR J2124-3358, and PSR J0030+0451) have lower X-ray luminosities (L_x $<10^{30}$ ergs s^{-1} at 1-10 keV), soft thermal X-ray spectra, and broad X-ray pulses. On the other hand, the Class-II members (PSR B1821-24, PSR J0218-4232, and PSR B1937+21) have higher X-ray luminosities (L_x $>10^{32}$ ergs s^{-1} at 1-10 keV), hard non-thermal X-ray spectra, and sharp X-ray pulses. Moreover, Class-II shows hard X-ray spectral tails up to 20 keV. The characteristics of Class-II members point to a non-thermal origin related to physical processes taking place in the magnetosphere of a MSP.

Because of their short period, small period derivatives ($\dot{P}$ $<10^{-17}$ s s^{-1}) as well as their evolutional history in the binary systems, MSPs form a distinctive group from normal pulsars. Thus, it is worth constructing a self-consistent electrodynamic model for high-energy emission from MSPs. Since the electrodynamic outer-gap models (Takata, Shibata & Hirotani 2004 ; Takata et al. 2006 ; Hirotani 2006) have applied the method only to young and middle-aged pulsars (e.g., Crab, Vela, Geminga), and used whole surface cooling neutron star thermal emission, we investigate the electrodynamic model of MSPs in this paper, evaluating the soft-photon field from the heated polar cap.

2. Electrodynamics of Particle Accelerator

2.1 Physical Processes

Spectral energy distributions (SEDs) offer

the key to an understanding of the radiation processes. Thompson et al. (1999) compiled a useful set of broad-band SED for the seven high-confidence γ-ray pulsars. The most striking feature of these νF_ν plots is the flux peak above 0.1 GeV with a turnover at several GeV. Various models (Daugherty & Harding 1982, 1996a,b; Romani and Yadigaroglu 1995; Romani 1996; Zhang & Cheng 1997; Higgins & Henriksen 1997, 1998; Hirotani & Shibata 1999a,b,c) conclude that these photons are emitted by the electrons or positrons accelerated above 5TeV via curvature process. In the outer magnetosphere of an ordinary pulsar, or in the entire magneto- sphere of a millisecond pulsar, such γ-rays materialize as pairs by colliding with ambient soft photons. For example, the curvature photons that have energies above GeV, efficiently materialize colliding with the surface thermal photons in keV energies. The replenished charges partially screen the original acceleration field, $E_\parallel$.

All these things make it clear that we have to solve the Poisson equation for the electro-static potential self-consistently with the Boltzmann equations for the created and injected $e^\pm$'s and for the inward- and outward-propagating γ-rays. In this paper, instead of solving the Boltzmann equations regarding the distribution functions of $e^\pm$'s and γ-rays continuous, we solve the motion of individual particles and γ-rays for simplicity, by introducing appropriate quanta, which represents the weight of particle number in the phase space. We could any time construct the distribution functions of $e^\pm$'s and γ-rays from the calculated motion of them.

In this paper, the Poisson equation is solved by the relaxation method. The motion of individual particles and γ-rays is calculated by Runge-Kutta method with adaptive stepsize control.

2.2 Poisson equation

The Poisson equation of the non-corotational potential ϕ is given by

$$\nabla^2\phi = -4\pi(\rho - \rho_{GJ}) \tag{1}$$

where the Goldreich-Julian charge density is defined as (Goldreich & Julian, 1969)

$$\rho_{GJ} = -\frac{\boldsymbol{\Omega}\cdot\boldsymbol{B}}{2\pi c} + \frac{(\boldsymbol{\Omega}\times\boldsymbol{r})\cdot(\nabla\times\boldsymbol{B})}{4\pi c} \tag{2}$$

The pulsar magnetosphere has no variation of non-corotational potential along the magnetic field lines (i.e., no potential drop), provided that $\rho = \rho_{GJ}$ holds in the entire region; that is, there exists a trivial solution, ϕ=constant, which value coincides with the boundary value. On the other hand, if ρ deviates from ρ_{GJ} in some region, $E_\parallel$ is exerted to accelerate particles.

2.3 particle equations of motion

The evolutions of momentum ($p \equiv |\boldsymbol{p}|$) and pitch angle ($\chi$) of a positron and an electron are described by

$$\frac{d}{dt}p = qE_\parallel \cos\chi - \frac{P_{sc}}{c} \tag{3}$$

$$\frac{d}{dt}\chi = \frac{qE_\parallel \sin\chi}{p} \tag{4}$$

$$\frac{d}{dt}s = \frac{p\cos\chi}{\sqrt{m_e^2 + (p/c)^2}} \tag{5}$$

where c is the speed of light and s is the distance along the magnetic field line. For positrons (or electrons), q=+e (or q=-e) is adopted, where e is

the magnitude of the charge on an electron. The radiation reaction force, P_{SC}/c, due to synchro-curvature radiation is given by (Zhang & Cheng 1997),

$$\frac{P_{SC}}{c} = \frac{e^2\Gamma^4 Q_2}{12 r_c}\left(1+\frac{7}{r_c^2 Q_2^2}\right) \quad (6)$$

where

$$r_c = \frac{c^2}{(r_B+\rho_c)(c\cos\chi/\rho_c)^2 + r_B\omega_B^2} \quad (7)$$

$$Q_2^2 = \frac{1}{r_B}\left(\frac{r_B^2+\rho_c r_B - 3\rho_c^2}{\rho_c^3}\cos^4\chi + \frac{3}{\rho_c}\cos^2\chi + \frac{1}{r_B}\sin^4\chi\right) \quad (8)$$

$$r_B = \frac{\Gamma m_e c^2 \sin\chi}{eB} \quad (9)$$

$$\omega_B = \frac{eB}{\Gamma m_e c} \quad (10)$$

where Γ is the Lorentz factor of charged particles and ρ_c is the curvature radius of the magnetic field line.

2.4 Two-photon pair creation rate

The electron-positron pairs are created via photon-photon pair creation. The creation rate $S_+(t, \boldsymbol{r}, \boldsymbol{p})$ for positrons and $S_-(t, \boldsymbol{r}, \boldsymbol{p})$ for electrons with momentum $\boldsymbol{p}$ at position $\boldsymbol{r}$ and time t is given by

$$S_\pm(t,\boldsymbol{r},\boldsymbol{p}) = \int_{-1}^{1} d\mu_c \int d\varepsilon_\gamma \int d\boldsymbol{k}\, \eta_{p\pm g}(\varepsilon_\gamma, \boldsymbol{r}, \boldsymbol{k}) \quad (11)$$

where the function g represents the γ-ray distribution function at energy $m_e c^2 \varepsilon_\gamma$, momentum $\boldsymbol{k}$, and position $\boldsymbol{r}$. The pair creation redistribution function η_p can be defined as

$$\eta_{p\pm}(\varepsilon_\gamma, \mu_c, \boldsymbol{p}, \boldsymbol{k}) = (1-\mu_c)\int_{\varepsilon_{th}}^{\infty} d\varepsilon_x \frac{dN_x}{d\varepsilon_x}\sigma_p(\varepsilon_\gamma, \varepsilon_x, \mu_c)\delta(\boldsymbol{p}-\boldsymbol{k}/2) \quad (12)$$

where μ_c is the cosine of the collision angle between the two photons, $\varepsilon_{th} \equiv 2/\left[(1-\mu_c)\varepsilon_\gamma\right]$ is the dimensionless threshold energy for a X-ray photon having energy $m_e c^2 \varepsilon_x$ to make a pair with the γ-ray having energy $m_e c^2 \varepsilon_\gamma$; σ_p refers to the pair-creation cross-section.

2.5 γ-ray emission, propagation, and absorption

The probability for a charged particle (with charge e) to emit photons via pure-curvature process is given by (Rybicki & Lightman 1979)

$$\eta_c = \frac{\sqrt{3}e^2\Gamma}{hR_c}\frac{1}{\varepsilon_\gamma}F\left(\frac{\varepsilon_\gamma}{\varepsilon_c}\right) \quad (13)$$

$$\varepsilon_c = \frac{1}{m_e c^2}\frac{3}{4\pi}\frac{hc\Gamma^3}{Rc} \quad (14)$$

$$F(s) = s\int_x^\infty K_{5/3}(t)dt \quad (15)$$

where ε_c is the critical energy of curvature radiation, R_c the curvature radius of the magnetic field line, and $K_{5/3}$ the modified Bessel function of the order 5/3.

A γ-ray photon is emitted tangential to the local magnetic field line. The photon propagates along a straight ray path because we assume the flat space-time geometry, which is a good approximation in the outer magnetosphere.

During the propagation, a γ-ray may collide with the thermal X-ray and be absorbed due to the pair creation process as described in the foregoing section. The absorption rate is given by

$$S_\gamma = -\int_{-1}^{1} d\mu_c \int_1^\infty d\Gamma\, \eta_p(\boldsymbol{r},\Gamma,\mu_c)\cdot g(\varepsilon_\gamma, \boldsymbol{r}, \boldsymbol{k}) \quad (16)$$

2.6 boundary conditions

We consider the situation that the lower boundary of the gap, $\theta_* = \theta_*^{\max}$, coincides with the last open field line. θ_* is the magnetic colatitude of the point where the magnetic field line intersects the stellar surface. We assume that

the upper boundary, $\theta_* = \theta_*^{\min}$, coincides with a particular magnetic field line between the last open field line and the magnetic axis. The thickness of the gap is defined as

$$h_m \equiv \frac{\theta_*^{\max} - \theta_*^{\min}}{\theta_*^{\max}} \quad (17)$$

We solve the Poisson equation from the neutron star surface to the outer magnetosphere. Thus, we define that the inner boundary coincides with the stellar surface. As for the *outer* boundary, we solve the Poisson equation to a large enough distance, $s = 1.4\varpi_{LC}$, which is located outside of the light cylinder. Since the structure of the outer-most part of the magnetosphere is highly unknown, we artificially set $E_{\|}$=0 if the distance from the rotation axis, ϖ, becomes greater than $0.90\varpi_{LC}$. Under this artificially suppressed $E_{\|}$ distribution in $\varpi > 0.90\varpi_{LC}$, we solve the Boltzmann equations for outward-migrating particles and γ-rays in $0<s<1.4\varpi_{LC}$. For inward-migrating particles and γ-rays, we solve only in $\varpi < 0.9\varpi_{LC}$.

To solve the Poisson equation, an elliptic-type partial differential equation, we impose ϕ=0 at the inner, lower, and upper boundaries, assuming that both the lower, and upper boundaries are grounded to the star. At the outer boundary, we impose $\partial\phi / \partial s = -E_{\|} = 0$.

3. Result

3.1 Time-dependent Simulation

It is, unfortunately, difficult to constrain the time-dependent feature of γ-ray emissions observationally, because the EGRET experiment detected one GeV photon every tens of thousand pulsar rotations. Taking advantage of this fact, all the high-energy emission theories from rotating neutron-star magnetospheres have concentrated on stationary analyses. This drives us to the question whether the particle accelerators are, indeed, stationary or not, which is still unsettled.

On these grounds, we solve the Poisson equation and time-dependent Boltzmann equations for electrons, positrons and gamma-ray photons self-consistently. By starting from a nearly vacuum solution, we find that the solution evolves to a stationary state in a wide range of pulsar parameters, such as period, P, period derivative $\dot{P}$, and magnetic inclination angle, α_i. We will demonstrate this new result, applying the method to millisecond pulsar parameters in the subsections below.

3.2 Stability of Outer-Magnetospheric Gaps

It is conjectured by Hirotani (2006) that an outer-magnetospheric gap is electrodynamically stable. In this subsection, we will examine this prediction by a time-dependent simulation. We start with the vacuum solution of $E_{\|}(s, \theta_*)$ with an injection of electrons at 1% of Goldreich-Julian rate, $0.01\ \Omega B / 2\pi$ [$\mathrm{cm^{-2}s^{-1}}$], across the outer boundary.

Such injected, inward-accelerated electrons emit copious curvature γ-rays, which efficiently collide with the surface X-rays to materialize as pairs in the inner magnetosphere. The created pairs discharge, partially screening the original $E_{\|}$. The discharged positrons are accelerated outwards, emitting curvature photons, some of which materialize in the outer magnetosphere. The

discharged electrons, on the other hand, emit inward-directed γ-rays, which efficiently cascade into higher generation pairs by head-on collisions with the surface X-rays.

If the created pair density becomes too large, the over-screened $E_{\parallel}$ results in a less-efficient γ-ray emission, leading to a decrease of pairs in a dynamical time scale, ϖ_{LC}/c. On the other hand, if the created pair density is too small, the under-screened $E_{\parallel}$ results in an increase of pairs. On these grounds, we can expect that an initial trial function evolves to the final, stationary solution after a lapse of several dynamical time scales.

In figure 1, we present the result of a stabilized solution: The heated polar-cap temperature settles down to the final value $kT \sim 153$ eV, after about 20 dynamical timescales. We adopted $P = 3.3$ ms, $\dot{P} = 6.2\times10^{-20}$ ss^{-1}, and $\alpha_i = 75°$, with $h_m = 0.9$.

We also find that this solution is marginally self-sustained in the sense that if one of the parameter is changed such as $P > 3.3$ ms, or $\dot{P} < 6.2\times10^{-20}$ ss^{-1}, or $\alpha_i < 75°$, or $h_m < 0.9$, the created current density evolves to a negligibly small value compared to the Goldreich-Julian value; in this case, the surface temperature is simply attributed to the injected particles across the outer boundary and kept below ~50 eV.

On the other hand, for a faster spin (i.e., $P < 3.3$ms), or larger magnetic moment (i.e., $\dot{P} > 6.2\times10^{-20}$ ss^{-1}), the final stable solution, with created current comparable to the Goldreich-Julian current and significantly greater than the injected current, has a higher polar-cap temperature, $kT > 153$ eV.

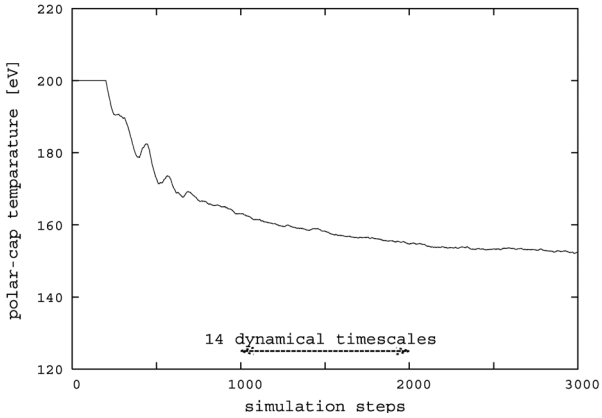

Fig. 1: The heated polar-cap temperature evolution.

3.3 Millisecond pulsar death line

Let us finally enlarge the electrodynamic consideration into the criterion for a gap to be self-sustained. If particles are efficiently accelerated and the resultant created current density, j_{gap}, is large enough, the electrons flowing onto the polar-cap surface will lead to a sufficient thermal emission from the surface. The efficient thermal photon flux ensures copious pair creation in the gap, and hence the large enough j_{gap} self-consistently.

However, if the external electric field, $E_{\parallel}$, decreases by some fictitious mechanism (e.g., by artificial decrease of neutron-star magnetic moment, μ), j_{gap} and hence the polar-cap temperature, kT, decrease. The decrease of the surface photon flux further decreases j_{gap}, which partially recovers the decrease of $E_{\parallel}$. However, if $E_{\parallel}$ is decreased (e.g., by the decrease of μ) too much, even the vacuum solution of $E_{\parallel}$ cannot maintain the pair creation cascade in the gap; in this case, j_{gap} as well as kT tends to vanish, remaining an in-active gap with the vacuum

potential drop.

Viewed in this light, we can define a 'death line' of the particle accelerator on $(P, \dot{P})$ plane, adopting some fixed value of α_i and h_m. If pair creation is insufficient, then the gap upper boundary will be located near the magnetic pole, because the upper boundary will be formed by the copiously created charges that freely moves along the field lines and screens $E_{\parallel}$. Thus, to find the death line, we adopt a large value of h_m = 0.9 in this subsection. As for α_i, we adopt two representative values, 60° and 75°.

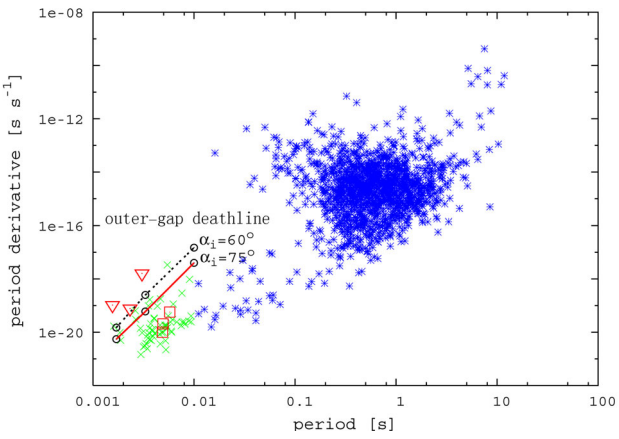

Fig. 2: P-$\dot{P}$ diagram of pulsars and millisecond deathline. Pulsars with period shorter than 10 ms are denoted by crosses. The dashed and solid lines denote the deathline for inclination angle 60 and 75 degree. The triangles denote the Class-II millisecond pulsars while the squares denote Class-I.

To determine the death line, we investigate the marginal value of $\dot{P}$ below which a self-sustained gap does not exist for a fixed value of P. For both cases, α_i = 60° and 75°, we adopt three fixed values of P, 1.7 ms, 3.3 ms, 10 ms. For α_i = 60°, we find that $\dot{P} > 1.5\times10^{-20}$ for P = 1.7 ms, $\dot{P} > 2.5\times10^{-19}$ for P = 3.3 ms, and $\dot{P} > 1.5\times10^{-17}$ for P = 10 ms. For α_i = 75°, on the other hand, $\dot{P} > 6.0\times10^{-21}$ for P = 1.7 ms, $\dot{P} > 6.0\times10^{-10}$ for P = 3.3 ms, and $\dot{P} > 4.0\times10^{-18}$ for P = 10 ms. These conditions are plotted on $(P, \dot{P})$ diagram in figure 2 with open circles. The inferred death lines from these six points are also shown in figure 2: the dashed line denotes the death line for α_i = 60° while the solid line for α_i = 75°.

It is noted that the death line for α_i =60° is located above that for α_i =75° on the $(P, \dot{P})$ plane. It means that for smaller α_i, the larger $\dot{P}$ is required for a self-sustained solution, provided that all other pulsar parameters (e.g., Ω, I, r_*) are fixed. The reason is described as follows:

- The null surface, where ρ_{GJ} vanishes (i.e., B_z=0), intersects the gap at lower altitudes for larger α_i.
- The inner boundary, which is located inside of the null surface, gets closer to the star with increasing α_i.
- The enhanced pair creation near the star because of the larger α_i, maintains the gap with smaller μ, and hence $\dot{P}$ for a fixed P.
- In addition to the enhanced pair creation due to the increase of soft photon density and due to the head-on collisions near the star, the potential drop increases with increasing longitudinal distance of the gap.

That is, both effects -- enhanced pair creation and increased potential drop due to a larger α_i -- help the gap be self sustained with a smaller $\dot{P}$.

It follows from figure 2 that the three Class II X-ray MSPs, denoted by triangles, appear above the two death lines. On the contrary, Class I

X-ray MSPs (squares) and most of other MSPs (crosses) are located below the death lines. Since the characteristics of Class-II members point to a non-thermal origin due to active particle acceleration taking place in the magnetosphere of a MSP, it is natural to interpret that the current calculation is associated with the Class-II MSPs. It would be possible to argue that the consistency of the obtained death line with the location of Class II MSPs on $(P, \dot{P})$ diagram support this interpretation of their non-thermal emission as a result of the self-sustained magnetospheric particle accelerator investigated in the present paper.

4. Conclusion

We study the high energy emission from pulsar magnetosphere and investigate the non-stationary particle acceleration in the outer-magnetospheric gap. Solving the Poisson equation and the time-dependent Boltzmann equations for electrons, positrons and γ-rays consistently on the two-dimensional poloidal plane, we compute the Lorentz factor and pitch angle evolution of the created particles, as well as the γ-ray emission, propagation and absorption.

We apply the method to millisecond pulsars, considering that the pair creation takes place due to the collisions between the γ-rays and the thermal photons emitted from the heated polar cap. The blackbody temperature of the heated polar cap is determined by the bombardment of back-flowing electrons. We find that self-sustained stationary solutions exist for a range of representative parameters of millisecond pulsars.

We show the deathlines of millisecond pulsars in P- $\dot{P}$ diagram for two different inclination angles, 60° and 75°. The determination of the position of the deathline depends on whether a self-sustained particle accelerator can be formed or not. The deathline for α_i = 60° lies above that for α_i = 75°. Moreover, all of the three known Class-II MSP members locate above the two deathlines, while most of the other MSPs locate below the deathlines.

Although only PSR J0218+4232, one of Class-II MSPs, has been detected pulsed γ-ray emission, the improved sensitivity of future γ-ray telescopes may enable the detection of the curvature radiation from several MSPs. There is room for further investigation of self-consistent particle accelerator models in the context of theoretical prediction and interpretation of γ-ray emission from individual millisecond pulsars. Three-dimensional extension is essential in order to incorporate the three-dimensional propagation of emitted γ-rays, which is necessary to quantitatively calculate the phase-resolved spectrum and the pulse profiles of the γ-rays.

Acknowledgements

We thank the referee for insightful comments on the manuscript. This work was supported by the National Science Council of the Republic of China with the grant NSC 94-2112-M-007-002.

References

Cheng, K. S., Ho, C., & Ruderman, M. 1986a, *ApJ*, 300, 500

Cheng, K. S., Ho, C., & Ruderman, M. 1986b, *ApJ*, 300, 522

Cheng, K. S., Ruderman, M., & Zhang, L. 2000, *ApJ*, 537, 964

Chiang, J., & Romani, R. W. 1992, *ApJ*, 400, 629

Chiang, J., & Romani, R. W. 1994, *ApJ*, 436, 754

Daugherty, J. K., & Harding, A. K. 1982, *ApJ*, 252, 337

Daugherty, J. K., & Harding, A. K. 1996, *ApJ*, 458, 278

Dermer, C. D., & Sturner, S. J. 1994, *ApJ*, 420, L75

Dyks, J., & Rudak, B. 2003, *ApJ*, 598, 1201

Goldreich, P. Julian, W. H. 1969, *ApJ*, 157, 869

Harding, A. K., Tademaru, E., & Esposito, L. S. 1978, *ApJ*, 225, 226

Higgins, M. G., Henriksen R. N. 1997, *MNRAS*, 292, 934

Higgins, M. G., Henriksen R. N. 1998, *MNRAS*, 295, 188

Hirotani, K. & Shibata, S. 1999a, *MNRAS*, 308, 54

Hirotani, K. & Shibata, S. 1999b, *MNRAS*, 308, 67

Hirotani, K. & Shibata, S. 1999c, *PASJ*, 51, 683

Hirotani, K., Harding, A. K., & Shibata, S. 2003, *ApJ*, 591, 334

Hirotani, K. 2006, *New Research on Astrophysics, Neutron Stars and Galaxy Clusters* (new book series), ed. L.~V.~Ross, (Nova Science Publishers, Inc.), Vol. 1, Chap. 1, pp. 1--37 (ISBN 1-60021-110-0)

Kuiper, L. et al. 2000, *A&A*, 359, 615

Romani, R. W., & Yadigaroglu, I. A. 1995, *ApJ*, 438, 314

Romani, R. W. 1996, *ApJ*, 470, 469

Rybicki, G. B.,Lightman, A. P., 1979, *Radiation processes on astrophysics*. Wiley, New York

Sturner, S. J., Dermer, C. D., & Michel, F. C. 1995, *ApJ*, 445, 736

Takata, J., Shibata, S., & Hirotani, K. 2004, *MNRAS*, 354, 1120

Takata, J., Shibata, S., Hirotani, K., & Chang, H.-K. 2006, *MNRAS*, 366, 1310

Thompson, D. J., Bailes, M., Bertsch, D. L., Cordes, J., D'Amico, N., Esposito, J. A., Finley, J., Hartman, R. C., et al. 1999, *ApJ*, 516, 297

Zhang, L. Cheng, K. S. 1997, *ApJ*, 487, 370